Multidecadal Co-variability of North Atlantic Sea Surface Temperature, African Dust, Sahel Rainfall and Atlantic Hurricanes

Chunzai Wang [1]
Shenfu Dong [1 & 2]
Amato T. Evan [3]
Gregory R. Foltz [1]
Sang-Ki Lee [1 & 2]

[1] NOAA Atlantic Oceanographic and Meteorological Laboratory
Miami, Florida

[2] Cooperative Institute for Marine and Atmospheric Studies
University of Miami
Miami, Florida

[3] Department of Environmental Sciences
University of Virginia
Charlottesville, Virginia

Revised to *J. Climate*

October 2011

Corresponding author address: Dr. Chunzai Wang, NOAA/Atlantic Oceanographic and Meteorological Laboratory, 4301 Rickenbacker Causeway, Miami, FL 33149.
E-mail: Chunzai.Wang@noaa.gov.

Abstract

Most studies of African dust and North Atlantic climate have been limited to the short time period since the satellite era (1980 onward), precluding the examination of their relationship on longer timescales. Here we use a new dust data set with the record extending back to the 1950s to show a multidecadal co-variability of North Atlantic SST and aerosol, Sahel rainfall, and Atlantic hurricanes. When the North Atlantic Ocean was cold from the late 1960s to the early 1990s, the Sahel received less rainfall and the tropical North Atlantic experienced high concentration of dust. The opposite was true when the North Atlantic Ocean was warm before the late 1960s and after the early 1990s. This suggests that a positive feedback exists between North Atlantic SST, African dust, and Sahel rainfall on multidecadal timescales. That is, a warm (cold) North Atlantic Ocean produces a wet (dry) condition in the Sahel and thus leads to low (high) concentration of dust in the tropical North Atlantic which in turn warms (cools) the North Atlantic Ocean via coupled processes. An implication of this study is that coupled climate models need to be able to simulate this aerosol-related feedback in order to correctly simulate climate in the North Atlantic. Additionally, it is found that dust in the tropical North Atlantic varies inversely with the number of Atlantic hurricanes on multidecadal timescales due to the multidecadal variability of both direct and indirect influences of dust on vertical wind shear in the hurricane main development region.

1. Introduction

Sea surface temperature (SST) variability of the North Atlantic Ocean on timescales longer than interannual mainly shows a multidecadal variation and a secular trend (Trenberth and Shea 2006). There is a debate on what causes these variations, i.e., the relative roles of anthropogenic global warming, aerosols, and natural variability in controlling North Atlantic SST variability (e.g., Enfield et al. 2001; Knight et al. 2005; Trenberth and Shea 2006; Mann and Emanuel 2006; Zhang et al. 2007; Ting et al. 2009; Ottera et al. 2010; Wang and Dong 2010; Chang et al. 2011). In this paper, we focus on the multidecadal variability of the North Atlantic SST – the Atlantic multidecadal oscillation (AMO) (e.g., Delworth and Mann 2000; Enfield et al. 2001). Here the AMO index is defined as the detrended North Atlantic SST anomalies over the region of 0°-60°N and from the east coast of the Americas to 0° longitude (Fig. 1a). The extended reconstructed SST data (Smith et al. 2008) from 1950 to 2008 show that the AMO was in the cold phase from the late 1960s to the early 1990s and in the warm phases before the late 1960s and after the early 1990s.

The AMO has footprints on many parts of the global oceans (Fig. 1b; Ottera et al. 2010). In addition to the basin-wide warming of the North Atlantic Ocean, the warm phase of the AMO is associated with warming in the western North and South Pacific Oceans and the tropical eastern Indian Oceans and cooling over the global Southern Oceans and in the subtropical northeastern Pacific Ocean. Opposite-signed SST anomalies occur for the cold phase of the AMO. The Atlantic SST regression shows a bipolar seesaw pattern or an inter-hemispheric gradient (Stocker 1998), supporting the hypothesis that the driving mechanism of the AMO involves fluctuations of the Atlantic meridional overturning circulation (AMOC) (e.g., Delworth and Mann 2000; Knight et al. 2005; Delworth et al. 2007). As the AMOC is enhanced, a

warming and a cooling will occur in the North and South Atlantic Oceans, respectively, and *vice versa* for a reduction of the AMOC.

AMO variability is associated with changes of climate and extreme events such as drought, flood and hurricane activity (e.g., Enfield et al. 2001; Goldenberg et al. 2001; McCabe et al. 2004; Bell and Chelliah 2006; Wang and Lee 2009). Previous studies have shown that it is mainly the tropical portion of the AMO that is relevant for climate since the climate response to the North Atlantic SST anomalies is primarily forced at the low latitudes (e.g., Lu and Delworth 2005; Sutton and Hodson 2007). Accordingly, the influence of the AMO on climate and hurricane activity may operate via atmospheric circulation changes induced by the SST anomalies in the tropical North Atlantic and Caribbean Sea (Vimont and Kossin 2007; Wang et al. 2008). Recently, Dunstone et al. (2011) used the HadCM3 coupled climate model to show that the North Atlantic subpolar gyre is a potentially important region for driving the tropical atmosphere by changing the tropical SST. It is therefore important to explore and understand the mechanisms that drive multidecadal variability in the tropical North Atlantic SST.

The present paper focuses on the relationships of mineral dust concentration in the tropical North Atlantic with North Atlantic SST variability and Atlantic hurricanes. Owing to the lack of long-term observations of dust over the Atlantic, most observational studies regarding mineral aerosols and North Atlantic climate have been limited to the short period since the satellite era (approximately 1980 onward). Although several modeling studies have explored the relationship between dust and climate on long-term periods (e.g., Mahowald et al. 2010), there is a high degree of disagreement in modeled dust emissions and transport between such models (Huneeus et al. 2010), underscoring the importance of observation-based studies. In this paper, we use a new dust data set, which extends back to the 1950s, to examine dust-related North

Atlantic SST variability on multidecadal timescales and propose a novel mechanism for North Atlantic SST variability. The paper is organized as follows. Section 2 briefly describes and introduces the data sets used in this study. Section 3 shows a multidecadal co-variability of SST and dust in the North Atlantic, rainfall in the Sahel, and Atlantic hurricanes. Section 4 presents the linkage between dust in the tropical North Atlantic and African dust. Section 5 infers a positive feedback between North Atlantic SST, African dust, and Sahel rainfall on multidecadal timescales, and gives a discussion and summary.

2. Data sets

Several observational and reanalysis data sets are used in this study. SST is from the NOAA extended reconstructed SST version 3 (Smith et al. 2008). The atmospheric reanalysis data sets include the National Centers for Environmental Prediction-National Center for Atmospheric Research (NCEP-NCAR) reanalysis (Kalnay et al. 1996), the European Center for Medium Range Weather Forecasting (ECMWF) Reanalysis Archive (ERA-40; Uppala et al. 2005), and the newly developed NOAA Earth System Research Laboratory (ESRL) 20th Century Reanalysis (20CR) (Compo et al. 2011). All of these data sets are monthly and we use them for the period from January 1950 to December 2008 except for the ERA-40. For the ERA-40 data set, we use the data from January 1958 to December 2001 since the original ERA-40 reanalysis is from September 1957 to August 2002.

The rainfall data set is from the Global Precipitation Climatology Centre (GPCC) Version 5. The monthly rainfall data are gridded from the complete GPCC station database with more than 70,000 different raingauge stations worldwide (Rudolf et al. 1994). The gridded land precipitation is available for the period 1901-2009 in spatial resolutions of 0.5°×0.5°, 1.0°×1.0°,

and 2.5°×2.5°. The rainfall data are available from ftp://ftp-anon.dwd.de/pub/data/gpcc/html/fulldata_download.html.

The extended dust aerosol optical depth (DAOD) over the tropical North Atlantic from 1955 to 2008 was derived from a simple model using modern and historical data from meteorological satellites and a proxy record for atmospheric dust (Evan and Mukhopadhyay 2010). Satellite data include aerosol optical thickness retrievals from the Advanced Very High Resolution Radiometer (AVHRR) Pathfinder Extended dataset (PATMOS-x) for the period 1982-2008 and the Moderate Resolution Imaging Spectroradiometer (MODIS) on board the Aqua satellite for the period 2002-2008. The proxy record for atmospheric dust is based on measurements of crustal helium-4 (^{4}He) flux from a Porites coral at a water depth of 5 m near Pedra de Lume on Sal Island (16°45'44"N, 22°53'23"W), part of the Cape Verde archipelago, for the period of 1955-1994 (Mukhopadhyay and Kreycik 2008). The resultant 54-year record of DAOD has a 1.0°×1.0° spatial resolution and a monthly temporal resolution, and covers the region 0°-30°N, 10°-65°W. Evan et al. (2011) showed that the DAOD time series is well correlated with the station dust time series observed on the island of Barbados (13°10'N, 59°30'W). Since the DAOD data set is longer than the station data in Barbados, we use the DAOD data to study multidecadal variation in this paper.

Tropical cyclone data are obtained from the National Hurricane Center (NHC) Hurricane Best Track Files (HURDAT) (http://www.nhc.noaa.gov/pastall.shtml) (Jarvinen et al. 1984). Here we examine the numbers of Atlantic hurricanes, defined as the number of tropical cyclones with lifetime maximum sustained 1-minute wind speeds of 64 kt or greater (Saffir-Simpson categories 1-5).

3. Co-variability of SST, dust, rainfall and hurricanes

Variations in Atlantic SST and its inter-hemispheric gradient have been recognized to contribute to drought after the 1970s in the Sahel, a region in Africa between the Saharan Desert and the rainforests of Central Africa and the Guinean Coast (e.g., Folland et al. 1986; Giannini et al. 2003). Figures 2a and 2b show that the Sahel rainfall anomalies co-vary with the AMO on multidecadal timescales. The warm (cold) phases of the AMO are associated with positive (negative) rainfall anomalies in the Sahel. Because both the SST and rainfall data extend back to the beginning of the 20th century, we can check the relationship over a long-term period. Figure 3 shows that the relationship between the AMO and Sahel rainfall still holds if the time series are extended for the entire 20th century.

More interestingly, the dust aerosol optical depth (DAOD) in the tropical North Atlantic, which is proportional to mass concentration and is a proxy for atmospheric dust content, is out of phase with the AMO and the Sahel rainfall anomalies (Fig. 2c). This relationship is consistent with the analysis of Foltz and McPhaden (2008b), which used the data from 1980-2006 to show trends of Sahel rainfall and dust during the most recent upswing of the AMO. The nearly six-decade data used here show that when the North Atlantic Ocean was cold during the late 1960s to the early 1990s, the Sahel received less rainfall and the tropical North Atlantic had high concentration of dust. The opposite was true for the warm phases of the AMO after the early 1990s and before the late 1960s. We smooth each time series with a 7-year running mean filter (the shading in Fig. 2) and calculate the correlations among these filtered indices. The maximum correlations of -0.87 and 0.85 occur when the Sahel rainfall leads the DAOD and AMO indices by one and two years, respectively, consistent with the findings of Prospero and Lamb (2003) in the case of DAOD and Sahel rainfall. The maximum correlation between the AMO and DAOD

indices is -0.67 with zero lag. We calculate the effective degree of freedom (Quenouille 1952; Medhaug and Furevik 2011) as: $N_E = N/(1+2R_{X1}R_{Y1}+2R_{X2}R_{Y2})$, where N is the number of data points for the time series of X and Y; R_{X1} or R_{Y1} is the autocorrelation at lag one; and R_{X2} or R_{Y2} is the autocorrelation at lag two. All of these correlations are statistically significant based on student's t-test (above 95% significant levels). Although a correlation cannot tell us the cause and effect, these values suggest that dust in the tropical North Atlantic is related to Sahel rainfall and the North Atlantic SST (Prospero and Lamb 2003; Evan et al. 2011).

To emphasize AMO-related variability, we have detrended all data (i.e., removed linear trends). We also plot the data with the linear trends included; that is, data that include the components of both global warming and the AMO (Figs. 4 and 5). A comparison of Fig. 1b and Fig. 4b indicates that the global warming signal is spread throughout most of the global oceans (Barnett et al. 2005). With the long-term linear trend included, the rainfall anomalies in the Sahel show negative anomalies during the warm phase of the AMO after the early 1990s (Fig. 5b). If we compare Fig. 5b with Fig. 2b, it suggests that the impacts of the warming trend and the AMO on rainfall in the Sahel are opposite in sign. That is, the warming trend is associated with a reduction of rainfall in the Sahel region, whereas the warm phase of the AMO after the early 1990s tends to increase Sahel rainfall. This is consistent with modeling results that show that global warming leads to drought over the Sahel and a positive AMO phase enhances Sahel rainfall (e.g., Held et al. 2005; Mohino et al. 2011). The long-term drying in the Sahel may also be caused by other factors such as sulphate aerosol forcing that may lead to the cooling of the northern tropical oceans and then a decrease in Sahel rainfall (e.g., Rotstayn and Lohmann 2002; Chang et al. 2011). The DAOD anomalies in Fig. 5c are almost identical to those in Fig. 2c, indicating that the DAOD data used here do not have a significant long-term linear trend.

The spatial rainfall patterns related to the AMO and dust aerosol in the tropical North Atlantic are shown in Fig. 6. A strong positive AMO-rainfall regression stands out in the Sahel region (Fig. 6a). This indicates that on multidecadal timescales the warm (cold) North Atlantic Ocean corresponds to more (less) rainfall in the Sahel as the positive AMO phase leads to a northward shift of the intertropical convergence zone (ITCZ) in the Atlantic (e.g., Zhang and Delworth 2006; Krebs and Timmermann 2007). Since the northward shift of the Atlantic ITCZ is associated with the anomalous moisture convergence in the lower troposphere and upward motion at 500-hPa (Fig. 6c) over the Sahel, Sahel rainfall is enhanced. Figure 6a also shows the significant rainfall patterns associated with the AMO from North America to equatorial South America, consistent with previous studies (e.g., Enfield et al. 2001; McCabe et al. 2004). The dust-rainfall regression shows that high (low) concentration of dust in the tropical North Atlantic is associated with less (more) rainfall in the Sahel on multidecadal timescales (Fig. 6b). For the data with the linear trend included, the positive AMO-rainfall regression in the Sahel region is largely reduced and almost disappeared (Fig. 7a) due to the offsetting effect of global warming. The rainfall pattern from the GPCC product is consistent with the independent NCEP-NCAR reanalysis that shows the disappearance of upward motion at 500-hPa in the Sahel (Fig. 7b). Thus, our analyses here suggest that global warming decreases rainfall in the Sahel, whereas the warm phase of the AMO after the early 1990s increases rainfall in the Sahel.

An interesting topic is the relationship between African dust and Atlantic hurricane activity. Evan et al. (2006) have demonstrated a strongly negative relation between interannual variations in Atlantic tropical cyclone days and atmospheric dust measured by satellite during the years of 1982-2005. Here we focus on the multidecadal variations by performing the 7-year running mean of all indices (the indices are detrended before the 7-year running mean). Figure

8a shows that dust in the tropical North Atlantic is highly related to the number of Atlantic hurricanes. When dust concentration in the tropical North Atlantic is high (low), the number of Atlantic hurricanes is less (more). The mechanism may be due to an increase (decrease) of tropospheric vertical wind shear in the hurricane main development region induced by high (low) concentration of dust in the tropical North Atlantic (Fig. 8b). Dust variability changes the meridional air temperature gradient via dust-radiation processes (e.g., the dust-related shortwave and longwave radiative heating) which, in turn, alters the strength of the zonal winds or the easterly jet (see next section) through the thermal wind balance and thus the vertical wind shear. Indeed, Chen et al. (2010) used a numerical model to show that dust-radiation processes do change vertical profiles of winds and temperatures.

The vertical wind shear variability may also be influenced by indirect effect of dust on atmospheric circulation. Dust concentration can affect other atmospheric and oceanic processes and then wind shear and hurricanes, such as Sahel rainfall (Landsea and Gray 1992), the Saharan air layer (Dunion and Velden 2004), and North Atlantic SST (Goldenberg et al. 2001). The vertical wind shear during the summer and fall in the hurricane main development region is also related to the Atlantic warm pool (Wang et al. 2006) and the Atlantic meridional mode (Vimont and Kossin 2007). Thus, it is possible that the coupled response of winds and SST to dust radiative forcing may act to reinforce the wind shear anomalies, via mechanisms described by Evan et al. (2011). All of these processes are not independent and can contribute to the changes of vertical wind shear. Further studies in this topic are needed.

4. African dust and dust in the tropical North Atlantic

Previous studies have suggested that Atlantic dust storm frequency and intensity changes

are related to or are likely to be partially forced by variability in Sahelian precipitation. For example, Prospero and Lamb (2003) used the data from 1965-1998 to show a negative correlation of Sahel rainfall with dust concentration observed on the island of Barbados in the western tropical North Atlantic during the following summer. Our analyses of Fig. 2 show that the Sahel rainfall anomalies are inversely related to dust in the tropical North Atlantic on multidecadal timescales. The question is: What is the mechanism for the negative relationship between Sahel rainfall and dust in the tropical North Atlantic on multidecadal timescales?

One possibility is that anomalously high precipitation causes a "greening" of the Sahel (Nicholson et al. 1998) and thus shrinking of dust source regions, increase in soil moisture, and decrease in surface shear stress acting on soils where vegetation is present (Marticorena et al. 1997). It is also possible that surface winds play an important role in dust production in the Sahel region. To examine the role of surface winds, we identify the high and low dust years by the top and bottom quartiles of the DAOD time series, respectively. We then calculate the composite wind difference between the high and low dust years. The composite wind map from the NCEP-NCAR reanalysis shows an increased surface wind speed across the Sahel, centered near 15°N, during periods of high DAOD in the tropical North Atlantic (Fig. 9a). An increase in surface wind speed over dust source regions such as the Bodélé Depression – the lowest point in Chad and the planet's largest single source of dust (Washington et al. 2006) – would lead to increased atmospheric dust loading since deflation is proportional to surface shear stress (Marticorena et al. 1997). Given the cubic sensitivity of dust mobilization to wind speed, a small change of winds is capable of large change in dust output from the Bodélé (Washington et al. 2009) and other source regions. To confirm the results, we repeat the calculations by using the ERA-40 reanalysis and the 20CR reanalysis (Figs. 9b and c). The band of highest wind speed is

shifted about 5 degrees north for the ERA-40 and 20CR, but overall the patterns are similar: an increased surface wind speed across the Sahel and thus more dust production in the Bodélé Depression.

The dust in the Bodélé Depression can be transported southwestward at low levels, and then vertical mixing and vertical motion can allow the easterly flows to transport it into the Atlantic. Washington et al. (2009) computed the transport pathways from the Bodélé Depression using a Lagrangian advection model driven by the 3-D ERA-40 reanalysis winds. They found that the path of the trajectories in the peak dust-production months could reach the Atlantic in 5 days. It has been shown previously that transport of Saharan dust westward from the African coast is most strongly correlated with winds at about 700-hPa (Kaufman et al. 2005a). We therefore use the NCEP-NCAR reanalysis to calculate the regression of wind at 700-hPa onto the DAOD time series (Fig. 10a). The regressed wind at 700-hPa shows that the maximum easterly wind anomalies are south of the maximum dust band between 10°-20°N. The position inconsistency suggests that the dust changes in the tropical North Atlantic could be more due to enhanced dust production in the Sahel and Saharan regions, as evidenced by the decrease in precipitation (Fig. 6b) and the increase in surface wind over these source regions (Fig. 9). If more dust production occurs over the Sahel and Saharan regions, then the tropical North Atlantic will experience higher dust concentration because of transport by the mean zonal winds. The mean zonal winds in West Africa are featured by the African easterly jet (AEJ) which is maximized near 600-hPa and 15°N (Fig. 10b) and is formed due to the temperature contrast between the Sahara and Gulf of Guinea (e.g., Cook 1999). Figure 10c shows that the strong easterly winds at 700-hPa associated with the AEJ are across the entire tropical North Atlantic between 10°N-20°N. This distribution of the mean winds is consistent with the maximum dust

band between 10°-20°N, indicating that if more dust is produced over the Sahel, the tropical North Atlantic will experience higher dust concentration due to transport by the mean zonal winds.

The low levels of the atmosphere north of the Gulf of Guinea coast are characterized by the summer monsoon westerly winds (Fig. 10b). Our composite wind difference between the high and low dust years shows surface easterly wind anomalies north of the Gulf of Guinea coast (Fig. 9a). This indicates that a high dust year in the tropical North Atlantic is associated with a weakening of the southwesterly monsoon flow, which in turn is connected to the observed decrease in Sahel precipitation (Giannini et al. 2003).

5. Discussion and summary

The observed results presented in this paper suggest that a feedback process between the AMO and dust in the tropical North Atlantic may operate through Sahel rainfall variability. An initially warm North Atlantic Ocean is associated with a northward shift of the Atlantic ITCZ and southwesterly surface wind anomalies, resulting in an increase of rainfall in the Sahel. The increased rainfall leads to an increase in vegetation across the Sahel (Nicholson et al. 1998) and a decrease in source regions for mineral aerosols (Mahowald 2007). Associated with the decrease of aerosols in arid regions of Africa is a decrease of atmospheric wind-blown dust over the tropical North Atlantic. This, in turn, is a positive feedback onto tropical North Atlantic SST via the aerosol direct effect (Foltz and McPhaden 2008a; Evan et al. 2009; Evan et al. 2011). Note that these papers showed that changes in dustiness in the tropical North Atlantic force a significant portion of the underlying SST variability on interannual to decadal timescales by changing the amount of solar radiation reaching the ocean's surface, and Evan et al. (2011)

demonstrated that the atmospheric response to the equatorially asymmetric cooling by dust will tend to reinforce the forced SST anomalies via the wind-evaporation-SST feedback. However, further studies are needed to quantify the impact of dust forcing on North Atlantic SST and to determine the processes controlling African dust emission on multidecadal timescales. In particular, coupled ocean-atmosphere-land models instead of ocean-only models are needed to address the issue.

Almost all coupled climate models have difficulty in simulating the magnitude and phase of the AMO (Knight 2009; Medhaug and Furevik 2011), and the reason may be that they are missing the positive dust-AMO feedback proposed here. For example, for the few model experiments included in the Coupled Model Intercomparison Project (CMIP) phase 3 database that include dust, dust concentration is prescribed and does not vary from one year to the next. Furthermore, model dust concentrations are strongly dependent upon the global surface area over which deflation occurs, and there is considerable model spread in global desert area in the future warming scenarios (Mahowald 2007). Lastly, examination of a suite of coupled model experiments show large disagreement in even the long-term mean dust emissions and transport (Huneeus et al. 2011). We thus propose that one way to examine the effectiveness of coupled models in the future CMIP database, of which some will include interactive dust, is to identify the extent to which the connection between AMO-like variability and Atlantic dust cover, as observed here, is reproduced in 20th Century experiments. Coupled climate models need to capture the aerosol-related feedback for a realistic climate simulation in the Atlantic.

African dust also affects cloudiness by changing condensation nuclei, the Saharan air layer and atmospheric vertical motion. For example, Kaufman et al. (2005b) used the MODIS satellite data to show that aerosols increase the coverage of shallow clouds in the tropical

Atlantic by increasing condensation nuclei and reduce the cloud droplet size. The aerosol-induced cloud cover change can in turn affect the tropical North Atlantic SST by changing the heat fluxes into the ocean. Thus, the indirect effect of aerosol on cloud acts in the same sense as the direct effect on the tropical North Atlantic SST.

In summary, this paper uses a relatively long-term dust data set to show a multidecadal co-variability of the AMO, dust in the tropical North Atlantic, rainfall in the Sahel and Atlantic hurricanes, and to propose a novel mechanism for North Atlantic SST variability on multidecadal timescales. During the cold phase of the AMO from the late 1960s to the early 1990s, the Sahel received less rainfall and the tropical North Atlantic experienced high concentration of dust. The opposite was true when the AMO were during the warm phases before the late 1960s and after the early 1990s. The observed results suggest that a positive feedback exists between North Atlantic SST, African dust, and Sahel rainfall on multidecadal timescales. An implication of this study is that coupled climate models need to be able to simulate this aerosol-related feedback in order to correctly simulate climate variability and change in the North Atlantic. In addition to the relationships with the AMO and Sahel rainfall, dust in the tropical North Atlantic also varies multidecadally with vertical wind shear in the hurricane main development region, helping to explain the inverse relationship between dust and the number of Atlantic hurricanes.

Acknowledgments. We thank three anonymous reviewers for their comments and suggestions that help improve the manuscript. This work was supported by grants from National Oceanic and Atmospheric Administration (NOAA) Climate Program Office, the base funding of NOAA Atlantic Oceanographic and Meteorological Laboratory (AOML), and a grant from National

Science Foundation. The findings and conclusions in this report are those of the author(s) and do not necessarily represent the views of the funding agency.

References

Barnett, T. P., D. W. Pierce, K. M. AchutaRao, P. J. Gleckler, B. D. Santer, J. M. Gregory, and W. M. Washington, 2005: Penetration of human-induced warming into the world's oceans. *Science*, **309**, 284-287.

Bell, G. D., and M. Chelliah, 2006: Leading tropical modes associated with interannual and multidecadal fluctuations in North Atlantic hurricane activity. *J. Clim.,* **19**, 590-612.

Chang, C.-Y., J. C. H. Chiang, M. F. Wehner, A. R. Friedman, R. Ruedy, 2011: Sulfate Aerosol Control of Tropical Atlantic Climate over the Twentieth Century. *J. Climate*, **24**, 2540–2555.

Chen, S.-H., S.-H. Wang, and M. Waylonis, 2010: Modification of Saharan air layer and environmental shear over the eastern Atlantic Ocean by dust-radiation effects. *J. Geophys. Res.*, **115**, D21202, doi:10.1029/2010JD014158.

Compo, G. P., and Co-authors, 2011: The twentieth century reanalysis project. *Quart. J. Roy. Meteor.,* 137, 1-28.

Cook, K. H., 1999: Generation of the African easterly jet and its role in determining West African precipitation. *J. Climate*, **12**, 11651184.

Delworth, T. L., and M. E. Mann, 2000: Observed and simulated multidecadal variability in the Northern Hemisphere. *Clim. Dyn.*, **16**, 661-676.

Delworth, T. L., R. Zhang and M. E. Mann, 2007: Decadal to centennial variability of the Atlantic from observations and models. In *Ocean Circulation: Mechanisms and Impacts, Geophysical Monograph Series 173*, Washington, DC, American Geophysical Union, 131-148.

Dunion, J. P., and C. S. Velden, 2004: The impact of the Saharan air layer on Atlantic tropical cylone activity. *Bll. Am. Meteorol. Soc.*, **85**, 353-365.

Dunstone, N. J., D. M. Smith, and R. Eade, 2011: Multi-year predictability of the tropical Atlantic atmosphere driven by the high latitude North Atlantic Ocean. *Geophys. Res. Lett.*, **38**, L14701, doi:10.1029/2011GL047949.

Enfield, D. B., A. M. Mestas-Nunez, and P. J. Trimble, 2001: The Atlantic Multidecadal Oscillation and its relationship to rainfall and river flows in the continental US. *Geophys. Res. Lett.*, **28**, 2077-2080.

Evan, A. T., J. Dunion, J. A. Foley, A. K. Heidinger, and C. S. Velden, 2006: New evidence for a relationship between Atlantic tropical cyclone activity and African dust outbreaks. *Geophys. Res. Lett.*, **33**, L19813, doi:10.1029/2006GL026408.

Evan, A. T., et al., 2009: The role of aerosols in the evolution of tropical North Atlantic Ocean temperature anomalies. *Science*, **324**, 778-781, doi:10.1126/Science.1167404.

Evan, A. T., and S. Mukhopadhyay, 2010: African Dust over the Northern Tropical Atlantic: 1955–2008. *J. Appl. Meteor. Climatol.*, **49**, 2213–2229.

Evan, A. T., G. R. Foltz, D. Zhang, and D. J. Vimont, 2011: Influence of African dust on ocean-atmosphere variability in the tropical Atlantic. *Nature Geoscience*, doi:10.1038/ngeo1276.

Folland, C. K., T. N. Palmer, and D. E. Parker, 1986: Sahel rainfall and worldwide sea temperatures, 1901-85. *Nature,* **320**, 602-607.

Foltz, G. R., and M. J. McPhaden, 2008a: Impact of Saharan dust on tropical North Atlantic SST. *J. Climate*, **21**, 5048-5060.

Foltz, G. R., and M. J. McPhaden, 2008b: Trends in Saharan dust and tropical Atlantic climate

during 1980–2006. *Geophys. Res. Lett.*, **35**, L20706, doi:10.1029/2008GL035042.

Goldenberg, S. B., C. Landsea, A. M. Mestas-Nunez, and W. M. Gray, 2001: The recent increase in Atlantic hurricane activity. *Science,* **293**, 474-479.

Held, I. M., T. L. Delworth, J. Lu, K. L. Findell, and T. R. Knutson, 2005: Simulation of Sahel drought in the 20th and 21st centuries. *Proc. Nat. Acad. Sci.*, **102**, 17891-17896.

Huneeus, N., et al., 2011: Global dust model intercomparison in AeroCom phase I. *Atmos. Chem. Phys.*, doi:10.5194/acp-11-7781-2011.

Jarvinen, B. R., C. J. Neumann, and M. A. Davis, 1984: A tropical cyclone data tape for the North Atlantic Basin, 1886– 1983: Contents, limitations, and uses, *NOAA Tech. Memo. NWS NHC 22*, 21 pp., Coral Gables, Fla.

Kalnay, E., and Co-authors, 1996: The NCEP/NCAR 40-year reanalysis project. *Bull. Am. Meteorol. Soc.*, **77**, 437-471.

Kaufman, Y. J., I. Koren, L. A. Remer, D. Tanré, P. Ginoux, and S. Fan, 2005a: Dust transport and deposition observed from the Terra-Moderate Resolution Imaging Spectroradiometer (MODIS) spacecraft over the Atlantic Ocean. *J. Geophys. Res.*, **110**, D10S12, doi:10.1029/2003JD004436.

Kaufman, Y. J., I. Koren, L. A. Remer, D. Rosenfeld, and Y. Rudich, 2005b: The effect of smoke, dust, and pollution aerosol on shallow cloud development over the Atlantic Ocean. *Proc. Nat. Acad. Sci.*, **102**, 11207-11212.

Knight, J. R., R. J. Allan, C. K. Folland, M. Vellinga, and M. E. Mann, 2005: A signature of persistent natural thermohaline circulation cycles in observed climate. *Geophys. Res. Lett.*, **32**, L20708. doi:10.1029/2005GL024233.

Knight, J. R., 2009: The Atlantic multidecadal oscillation inferred from the forced climate

response in coupled general circulation models. *J. Clim.,* **22**, 1610-1625.

Krebs, U., and A. Timmermann, 2007: Tropical air-sea interactions accelerate the recovery of the Atlantic Meridional Overturning Circulation after a major shutdown. *J. Clim.,* **20**, 4940–4956.

Landsea, C. W., and W. M. Gray, 1992: The strong association between westen Sahelian monsoon rainfall and intense Atlantic hurricanes. *J. Climate*, **5**, 435-453.

Lu, J., and T. L. Delworth, 2005: Oceanic forcing of the late 20th century Sahel drought. *Geophys. Res. Lett.*, **32**, L22706, doi:10.1029/2005GL023316.

Mahowald, N. M., 2007: Anthropocene changes in desert area: Sensitivity to climate model predictions. *Geophys. Res. Lett.,* **34**, L18817, doi:10.1029/2007GL030472.

Mahowald, N. M., and Co-authors, 2010: Observed 20th century desert dust variability: Impact on climate and biogeochemistry. *Atmos. Chem. Phys.*, **10**, 10875-10893.

Mann, M. E., and K. A. Emanuel, 2006: Atlantic hurricane trends linked to climate change. *Eos Trans. AGU,* **87**, 233-244, doi:10.1029/2006EO240001.

Marticorena, B., G. Bergametti, B. Aumont, Y. Callot, C. N'Doume, and M. Legrand, 1997: Modeling the atmospheric dust cycle: 2. Simulation of Saharan dust sources. *J. Geophys. Res.,* **102**, 4387-4404.

McCabe, G., M. Palecki, and J. Betancourt, 2004: Pacific and Atlantic Ocean influences on multidecadal drought frequency in the United States. *Proc. Nat. Acad. Sci.*, **101**, 4136-4141.

Medhaug, I., and T. Furevik, 2011: North Atlantic 20th century multidecadal variability in coupled climate models: sea surface temperature and ocean overturning circulation. *Ocean Sci.*, **7**, 389-404.

Mohino, E., S. Janicot, and J. Bader, 2011: Sahel rainfall and decadal to multidecadal sea surface temperature variability. *Clim. Dyn.*, **37**, 419-440.

Mukhopadhyay, S., and P. Kreycik, 2008: Dust generation and drought patterns in Africa from helium-4 in a modern Cape Verde coral. *Geophys. Res. Lett.*, **35**, L20820, doi:10.1029/2008GL035722.

Nicholson, S. E., C. J. Tucker, and M. B. Ba, 1998: Desertification, drought, and surface vegetation: An example from the West African Sahel. *Bull. Amer. Meteor. Soc.*, **79**, 815–829.

Ottera, O. H., Bentsen, M., Drange, H., and Suo, L., 2010: External forcing as a metronome for Atlantic multidecadal variability. *Nature Geosci.*, **3**, 688-694.

Prospero, J. M., and P. J. Lamb, 2003: African droughts and dust transport to the Caribbean: Climate change implications. *Science,* **302**, 1024-1027.

Quenouille, M. H., 1952: *Associated measurements*. Butterworths Scientific Publications, London, 242 pp.

Rotstayn, L. D. and U. Lohmann, 2002: tropical rainfall trends and the indirect aerosol effect. *J. Climate*, **15**, 2103-2116.

Rudolf, B., H. Hauschild, W. Ruth, and U. Schneider, 1994: Terrestrial precipitation analysis: Operational method and required density of point measurements. *Global Precipitation and Climate Change*, M. Dubois and M. Desalmand, Eds., Springer-Verlag, 173–186.

Smith, T. M., R.W. Reynolds, T. C. Peterson, and J. Lawrimore, 2008: Improvements to NOAA's historical merged land-ocean surface temperature analysis (1880-2006). *J Clim.,* **21**, 2283-2296.

Sutton, R. T., and D. L. R. Hodson, 2007: Climate response to basin-scale warming and cooling

of the North Atlantic Ocean. *J. Climate*, **20**, 891-907.

Ting, M., Y. Kushnir, R. Seager, and C. Li, 2009: Forced and internal twentieth-century SST trends in the North Atlantic. *J. Climate*, **22**, 1469-1481.

Trenberth, K. E., and D. J. Shea, 2006: Atlantic hurricanes and natural variability in 2005. *Geophys. Res. Lett.,* **33**, L12704, doi:10.1029/2006GL026894.

Uppala S. M., and Co-authors, 2005: The ERA-40 re-analysis. *Q. J. R. Meteorol. Soc.,* **131**, 2961–3012.

Vimont, D. J., and J. P. Kossin, 2007: The Atlantic Meridional Mode and hurricane activity. *Geophys. Res. Lett.*, **34**, L07709, doi:10.1029/2007GL029683.

Wang, C., D. B. Enfield, S.-K. Lee, and C. W. Landsea, 2006: Influences of the Atlantic warm pool on Western Hemisphere summer rainfall and Atlantic hurricanes. *J. Climate,* **19**, 3011-3028.

Wang, C., S.-K. Lee, and D. B. Enfield, 2008: Atlantic warm pool acting as a link between Atlantic multidecadal oscillation and Atlantic tropical cyclone activity. *Geochem. Geophys. Geosyst.*, **9**, Q05V03, doi:10.1029/2007GC001809.

Wang, C., and S.-K. Lee, 2009: Co-variability of tropical cyclones in the North Atlantic and the eastern North Pacific. *Geophy. Res. Lett.,* **36**, L24702, doi:10.1029/2009GL041469.

Wang, C., and S. Dong, 2010: Is the basin-wide warming in the North Atlantic Ocean related to atmospheric carbon dioxide and global warming? *Geophys. Res. Lett.*, **37**, L08707, doi:10.1029/2010GL042743.

Washington, R., et al., 2006: Links between topography, wind, deflation, lakes and dust: The case of the Bodélé Depression, Chad. *Geophys. Res. Lett.,* **33**, L09401, doi:10.1029/2006GL025827.

Zhang, R., and T. L. Delworth, 2006: Impact of Atlantic multidecadal oscillations on India/Sahel rainfall and Atlantic hurricanes. *Geophys. Res. Lett.*, **33**, L17712,doi:10.1029/2006GL026267.

Zhang, R., T. L. Delworth, and I. Held, 2007: Can the Atlantic Ocean drive the observed multidecadal variability in Northern Hemisphere mean temperature? *Geophys. Res. Lett.*, **34**, L02709, doi:10.1029/2006GL028683.

Figure captions

Figure 1. The AMO index and its relationship with global ocean SST. Shown are (a) the detrended annual SST anomalies (°C) in the North Atlantic of 0°-60°N and from the east coast of the Americas to 0° longitude and (b) regression (°C per °C) of global annual SST anomalies onto the AMO index of (a). The regression is calculated based on the 7-year running mean data. The shading in (a) represents the 7-year running mean time series. The only regression exceeding the 95% significant level is plotted in (b).

Figure 2. The AMO, Sahel rainfall and dust in the tropical North Atlantic. Shown are (a) the AMO index (°C), (b) the annual rainfall anomalies (mm/month) in the Sahel (10°N-20°N, 20°W-40°E), and (c) the annual DAOD anomalies in the tropical North Atlantic (0°-30°N, 10°W-65°W). The shading represents the time series of 7-year running means.

Figure 3. The AMO index and Sahel rainfall time series for a long-term record of 1900-2008. Shown are (a) the AMO index (°C) and (b) the annual rainfall anomalies (mm/month) in the Sahel (10°N-20°N, 20°W-40°E). The time series are detrended and the shading represents the time series of 7-year running means.

Figure 4. The time series of the North Atlantic SST anomalies and its regressed map using the data with the linear trends included. Shown are (a) the annual SST anomalies (°C) in the North Atlantic of 0°-60°N and from the east coast of the Americas to 0° longitude and (b) regression (°C per °C) of global annual SST anomalies onto the North Atlantic SST index of (a). The

regression is calculated based on the 7-year running mean data. The only regression exceeding the 95% significant level is plotted. The shading in (a) represents the time series of 7-year running means.

Figure 5. The time series of the North Atlantic SST, Sahel rainfall and dust in the tropical North Atlantic using the data with the linear trends included. Shown are (a) the annual SST anomalies (°C) in the North Atlantic of 0°-60°N and from the east coast of the Americas to 0° longitude, (b) the annual rainfall anomalies (mm/month) in the Sahel (10°N-20°N, 20°W-40°E), and (c) the annual DAOD anomalies in the tropical North Atlantic (0°-30°N, 10°W-65°W). The shading represents the time series of 7-year running means.

Figure 6. Linkage of the AMO, rainfall and aerosol. Shown are (a) regression (mm/month per °C) of annual rainfall anomalies onto the AMO index, (b) regression (mm/month per DAOD) of annual rainfall anomalies onto the DAOD time series in the tropical North Atlantic, and (c) regression (Pa/s per °C) of annual 500-hPa vertical pressure velocity anomalies onto the AMO index. The regressions are calculated based on the 7-year running mean data. The only regressions exceeding the 95% significant level are plotted.

Figure 7. Linkage of the North Atlantic SST with rainfall using the data with the linear trends included. Shown are (a) regression (mm/month per °C) of annual rainfall anomalies onto the North Atlantic SST index and (b) regression (Pa/s per °C) of annual 500-hPa vertical pressure velocity anomalies onto the North Atlantic SST index. The regressions are calculated based on the 7-year running mean data. The only regression exceeding the 95% significant level is

plotted.

Figure 8. Relationships of dust with Atlantic hurricanes and vertical wind shear (VWS). Shown are (a) the time series of DAOD and the number of Atlantic hurricanes and (b) the time series of DAOD and VWS. The VWS is calculated as the magnitude of the vector difference between winds at 200-hPa and 850-hPa in the main development region of 85°W-15°W, 10°N-20°N during the hurricane season of June-November. To emphasize the multidecadal variability, we first detrend all indices and then perform a 7-year running mean filter to the indices. The correlations of dust with the number of hurricanes and VWS at zero lag are -0.79 and 0.69, respectively.

Figure 9. Composite surface wind differences between the high and low dust years. Shown are from (a) the NCEP-NCAR reanalysis, (b) the ERA-40 reanalysis and (c) the 20CR reanalysis. The shading represents the wind speed (m/s). The top and bottom quartiles of the DAOD time series are identified as the high and low dust years, respectively. For the NCEP-NCAR and 20CR, the 13 high dust years are 1962, 1973, 1974, 1975, 1979, 1981, 1983, 1984, 1985, 1986, 1987, 1988 and 1991; and the 13 low dust years are 1955, 1956, 1957, 1958, 1961, 1964, 1976, 1977, 1996, 2003, 2004, 2005, and 2006. For the ERA-40, the 11 high dust years are 1962, 1973, 1974, 1975, 1979, 1981, 1983, 1984, 1985, 1986 and 1987; and the 11 low dust years are 1958, 1961, 1964, 1965, 1968, 1976, 1977, 1993, 1995, 1996 and 2001. The green dot in (a) represents the Bodélé Depression – the lowest point in Chad and the planet's largest single source of dust.

Figure 10. Wind variations with dust and the mean winds. Shown are (a) regression (m/s per DAOD) of annual wind anomalies at 700-hPa onto the DAOD time series, (b) vertical-latitude section of the mean zonal wind at 0° longitude during July-September, and (c) the mean winds (vector) and the mean zonal winds (shading) at 700-hPa during July-September. The regression is calculated based on the detrended and 7-year running mean data. The only regressions exceeding the 95% significant level are plotted.

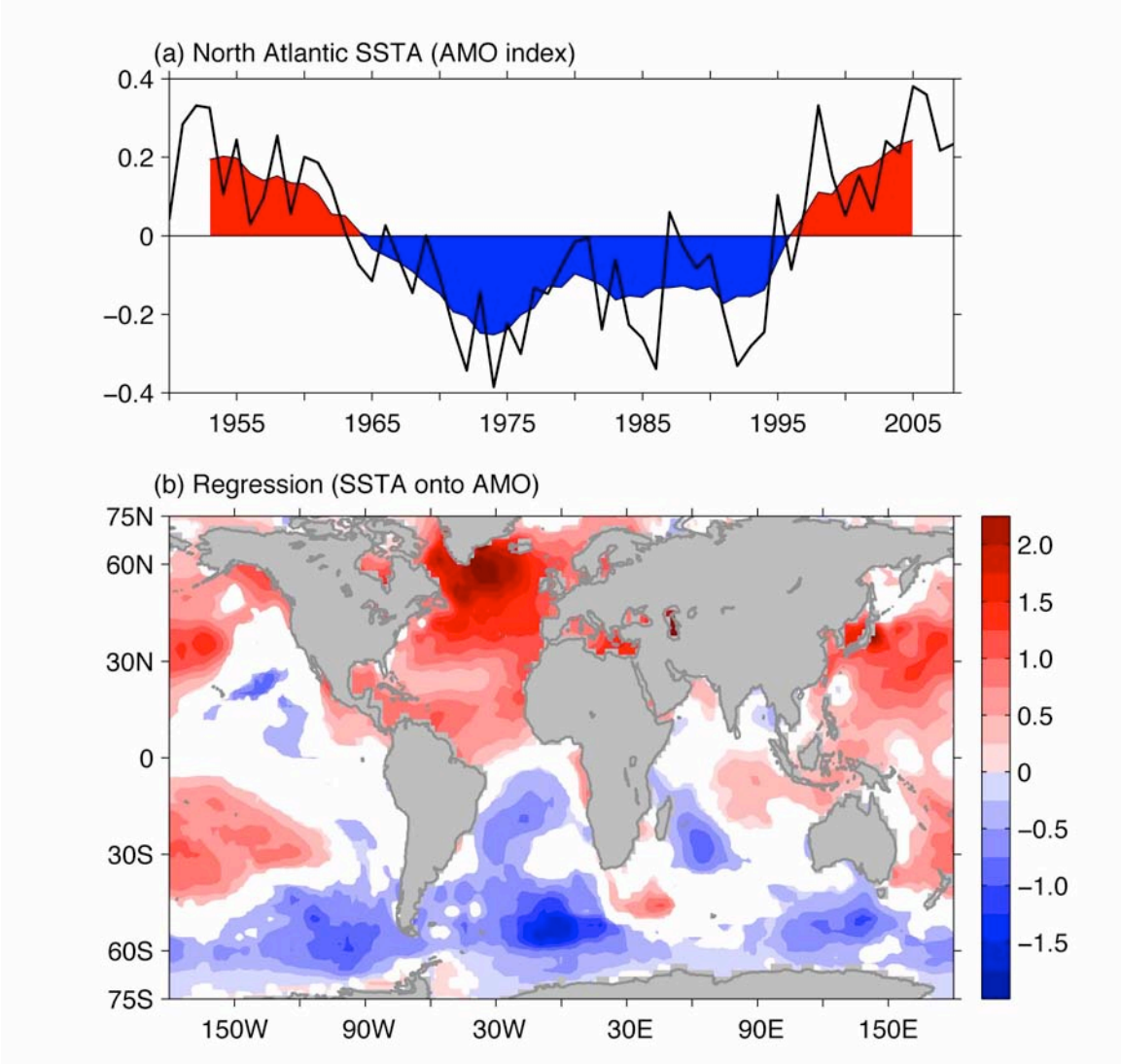

Figure 1. The AMO index and its relationship with global ocean SST. Shown are (a) the detrended annual SST anomalies (°C) in the North Atlantic of 0°-60°N and from the east coast of the Americas to 0° longitude and (b) regression (°C per °C) of global annual SST anomalies onto the AMO index of (a). The regression is calculated based on the 7-year running mean data. The shading in (a) represents the 7-year running mean time series. The only regression exceeding the 95% significant level is plotted in (b).

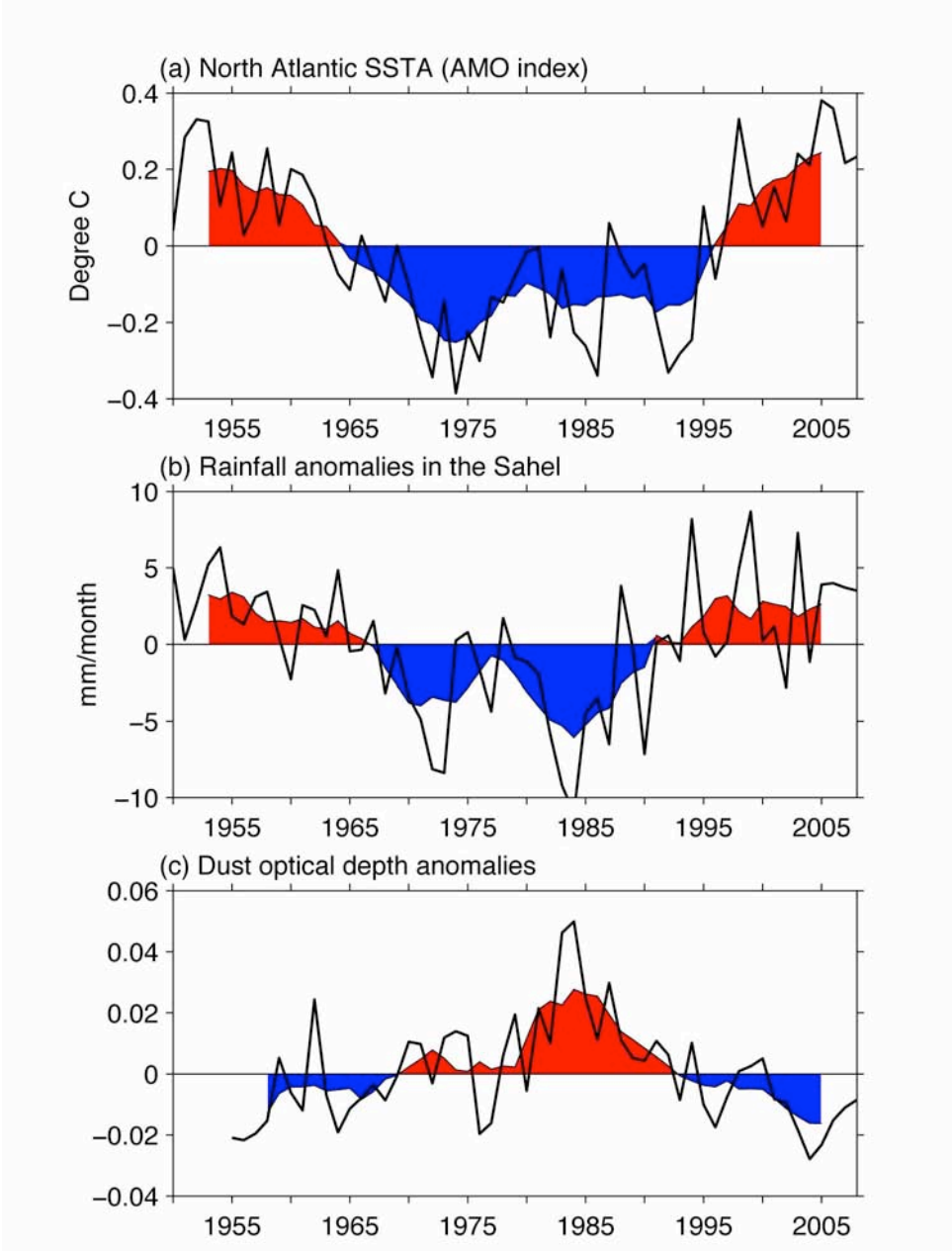

Figure 2. The AMO, Sahel rainfall and dust in the tropical North Atlantic. Shown are (a) the AMO index (°C), (b) the annual rainfall anomalies (mm/month) in the Sahel (10°N-20°N, 20°W-40°E), and (c) the annual DAOD anomalies in the tropical North Atlantic (0°-30°N, 10°W-65°W). The shading represents the time series of 7-year running means.

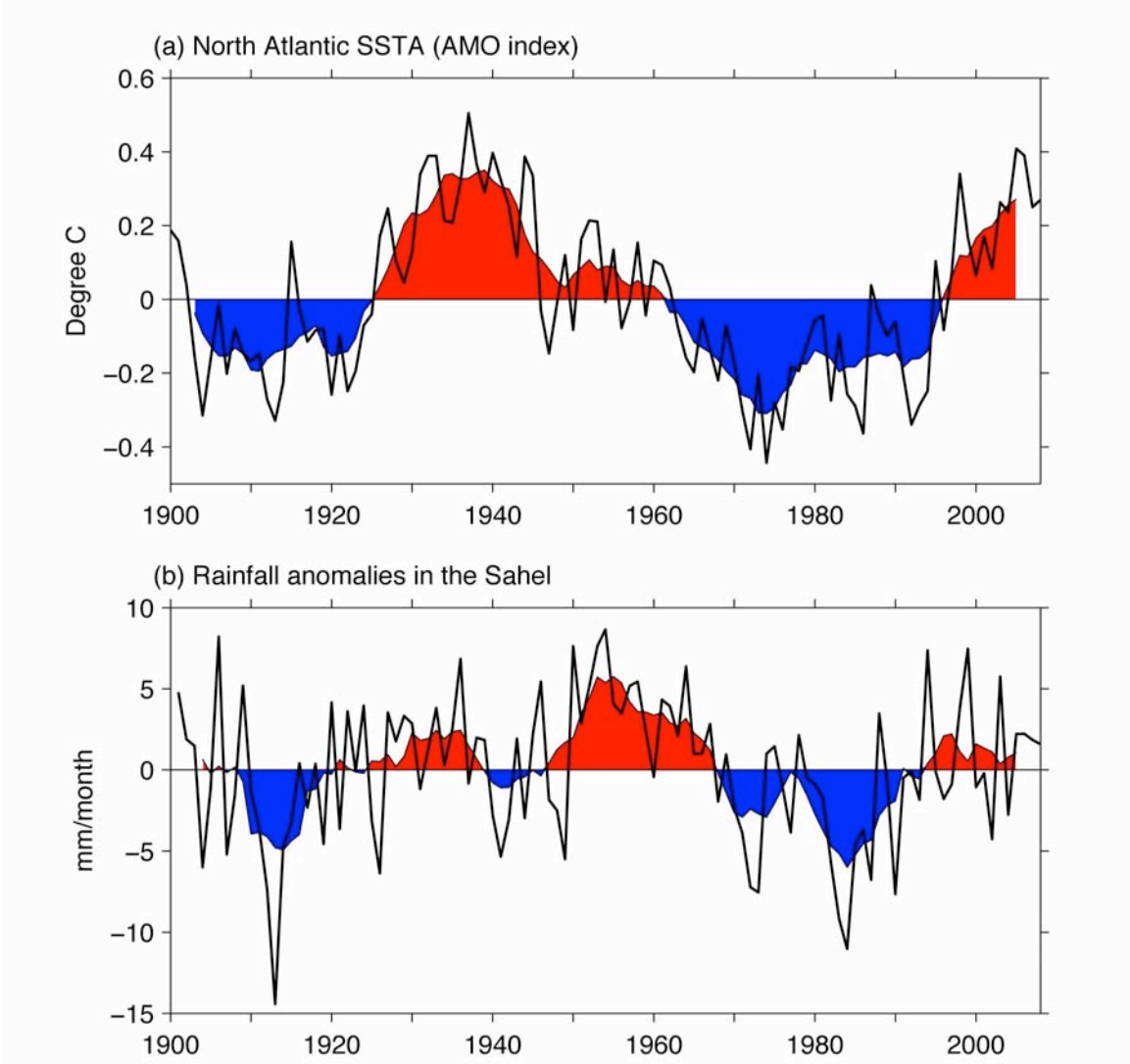

Figure 3. The AMO index and Sahel rainfall time series for a long-term record of 1900-2008. Shown are (a) the AMO index (°C) and (b) the annual rainfall anomalies (mm/month) in the Sahel (10°N-20°N, 20°W-40°E). The time series are detrended and the shading represents the time series of 7-year running means.

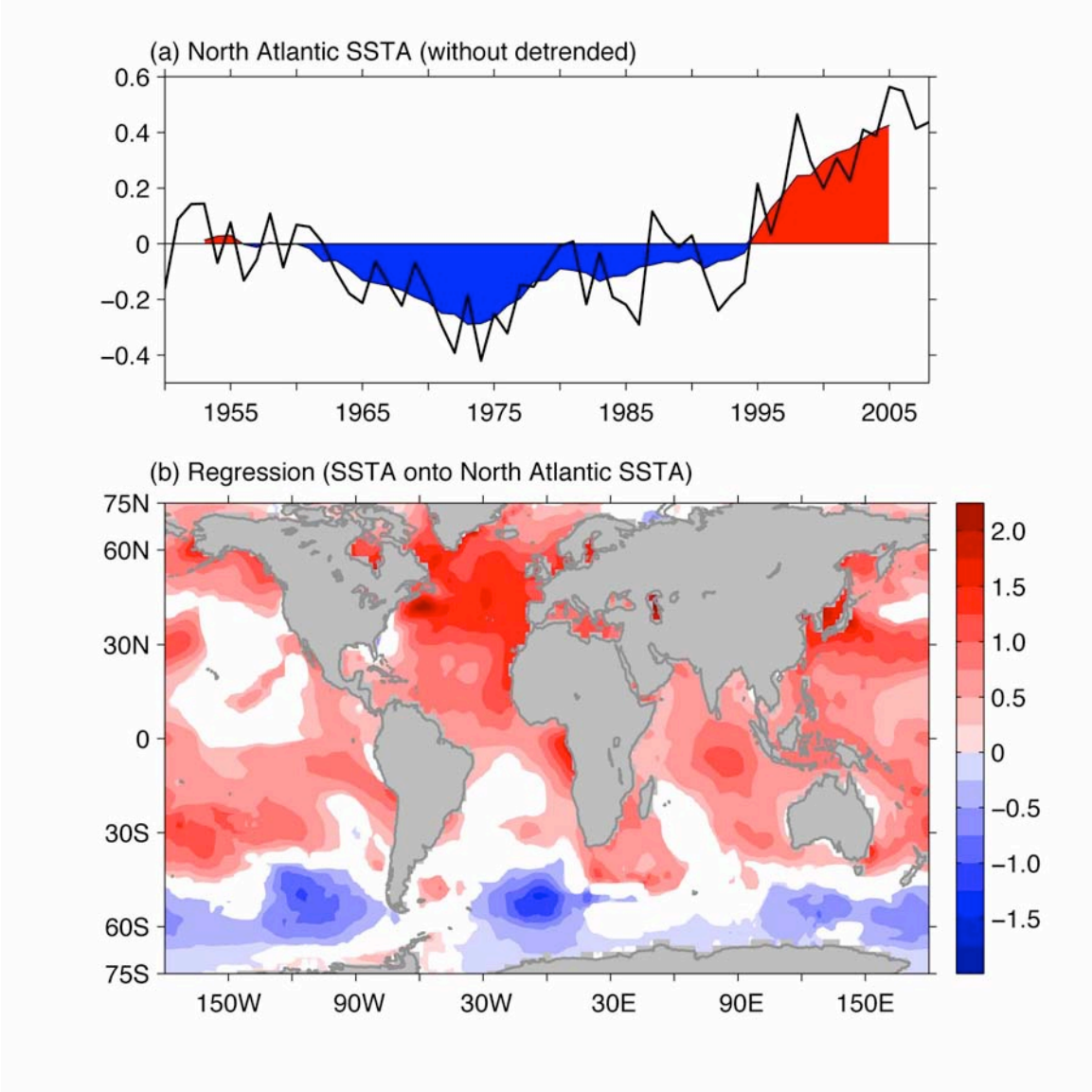

Figure 4. The time series of the North Atlantic SST anomalies and its regressed map using the data with the linear trends included. Shown are (a) the annual SST anomalies (°C) in the North Atlantic of 0°-60°N and from the east coast of the Americas to 0° longitude and (b) regression (°C per °C) of global annual SST anomalies onto the North Atlantic SST index of (a). The regression is calculated based on the 7-year running mean data. The only regression exceeding the 95% significant level is plotted. The shading in (a) represents the time series of 7-year running means.

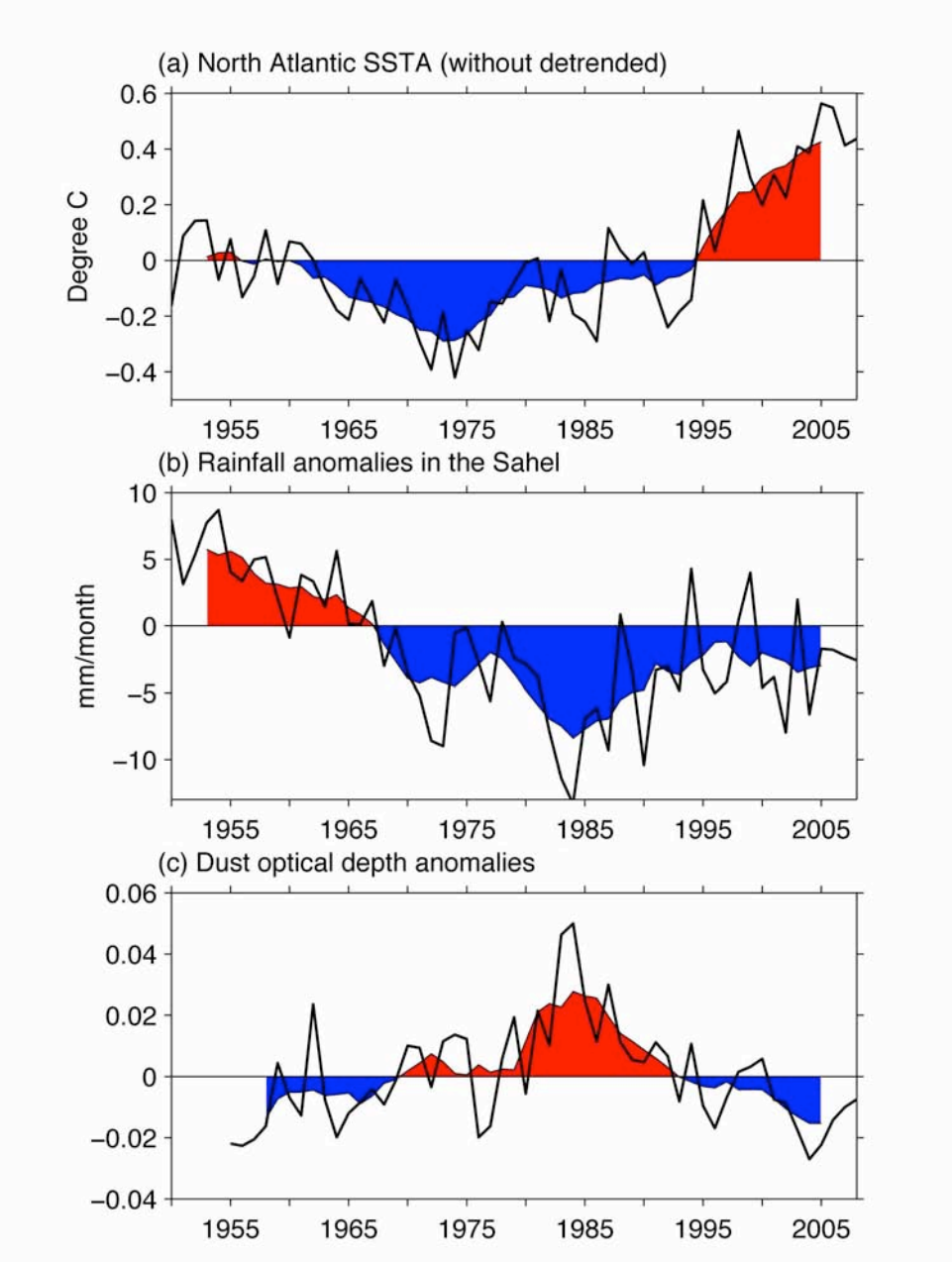

Figure 5. The time series of the North Atlantic SST, Sahel rainfall and dust in the tropical North Atlantic using the data with the linear trends included. Shown are (a) the annual SST anomalies (°C) in the North Atlantic of 0°-60°N and from the east coast of the Americas to 0° longitude, (b) the annual rainfall anomalies (mm/month) in the Sahel (10°N-20°N, 20°W-40°E), and (c) the annual DAOD anomalies in the tropical North Atlantic (0°-30°N, 10°W-65°W). The shading represents the time series of 7-year running means.

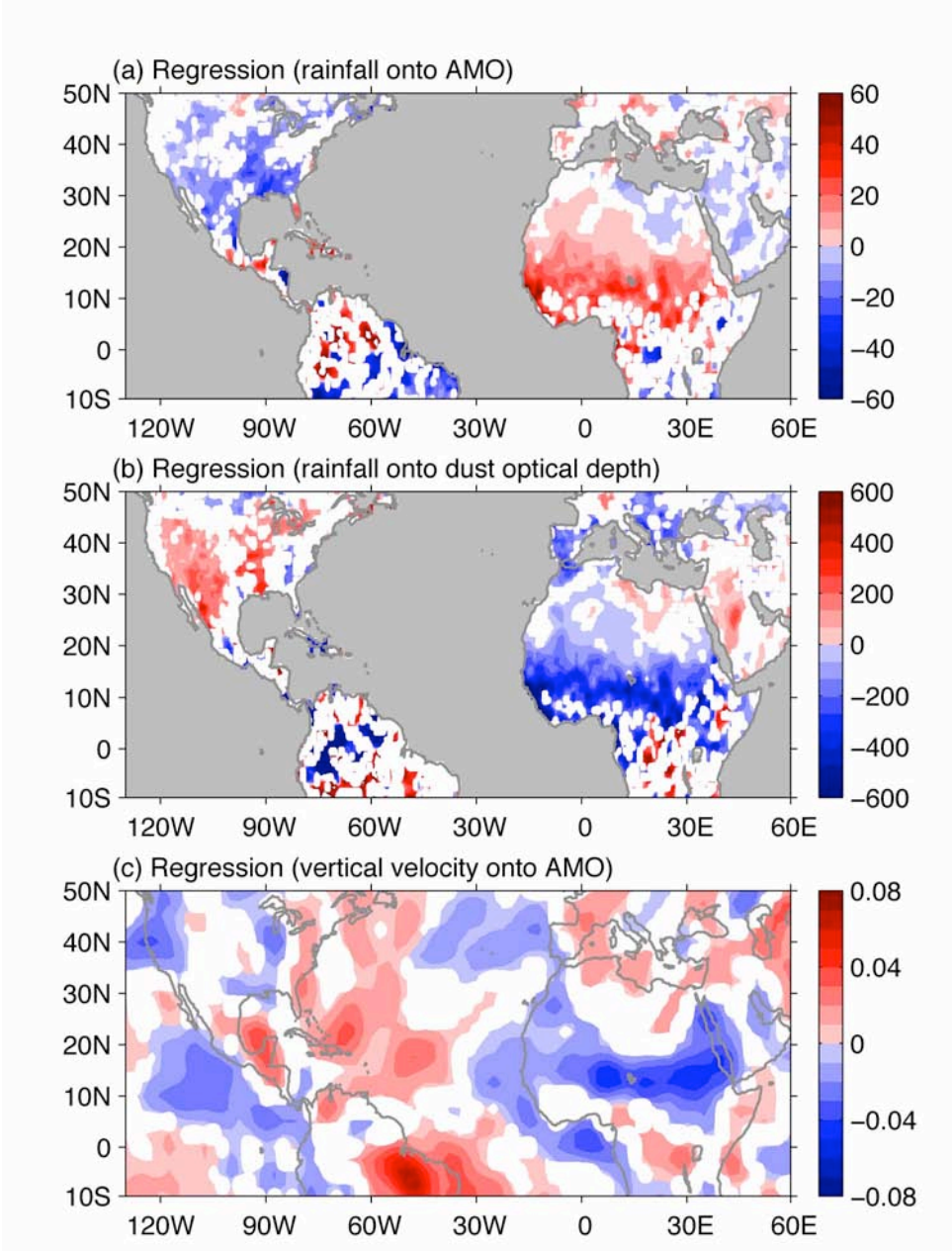

Figure 6. Linkage of the AMO, rainfall and aerosol. Shown are (a) regression (mm/month per °C) of annual rainfall anomalies onto the AMO index, (b) regression (mm/month per DAOD) of annual rainfall anomalies onto the DAOD time series in the tropical North Atlantic, and (c) regression (Pa/s per °C) of annual 500-hPa vertical pressure velocity anomalies onto the AMO index. The regressions are calculated based on the 7-year running mean data. The only regressions exceeding the 95% significant level are plotted.

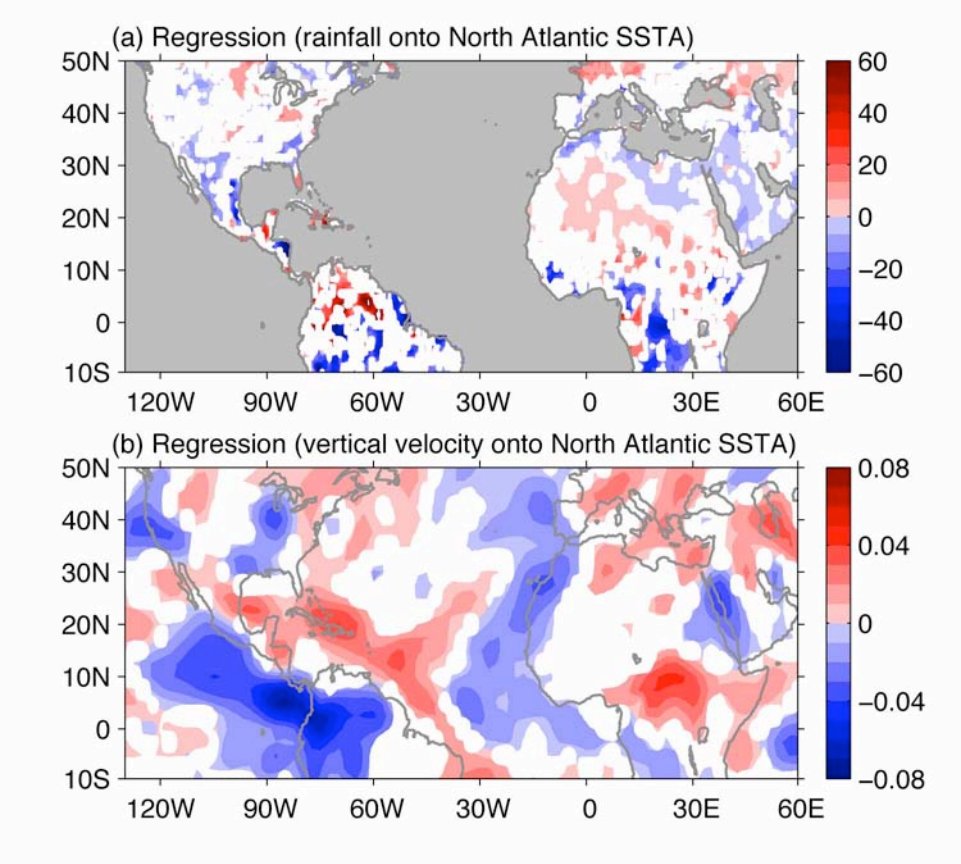

Figure 7. Linkage of the North Atlantic SST with rainfall using the data with the linear trends included. Shown are (a) regression (mm/month per °C) of annual rainfall anomalies onto the North Atlantic SST index and (b) regression (Pa/s per °C) of annual 500-hPa vertical pressure velocity anomalies onto the North Atlantic SST index. The regressions are calculated based on the 7-year running mean data. The only regression exceeding the 95% significant level is plotted.

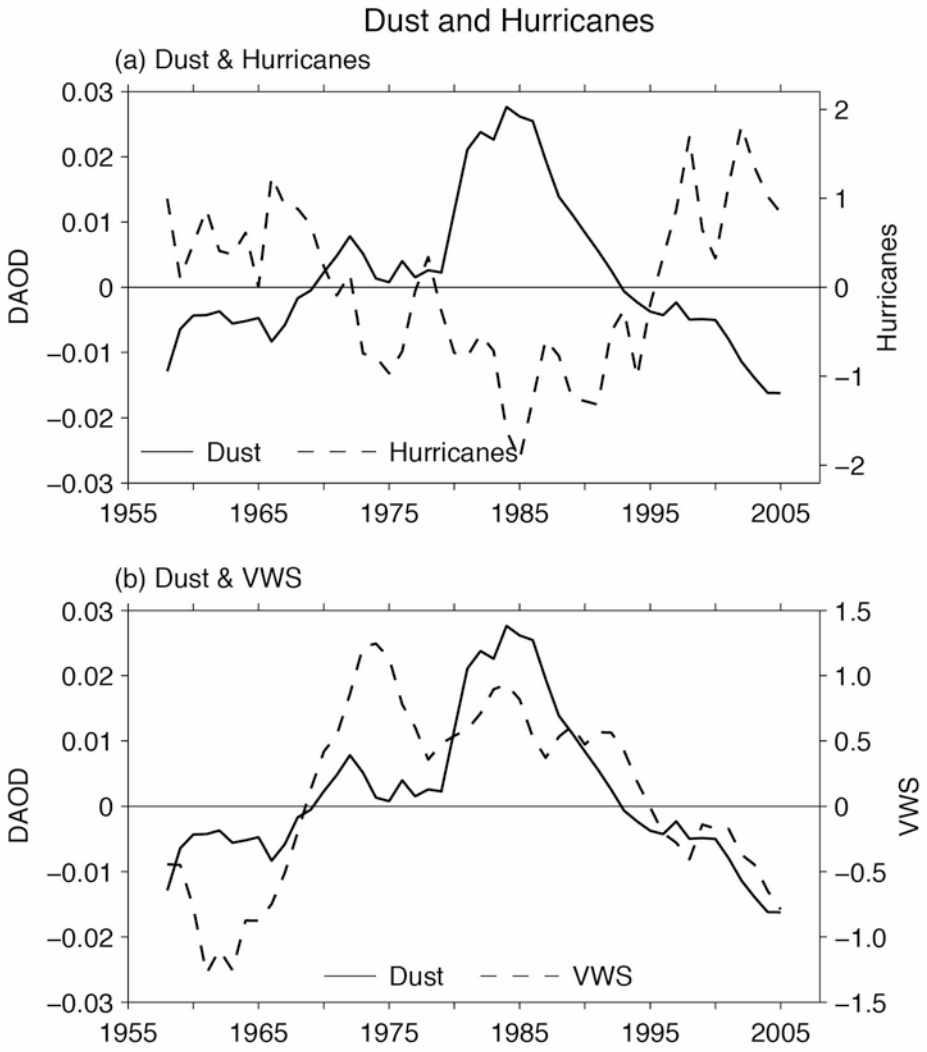

Figure 8. Relationships of dust with Atlantic hurricanes and vertical wind shear (VWS). Shown are (a) the time series of DAOD and the number of Atlantic hurricanes and (b) the time series of DAOD and VWS. The VWS is calculated as the magnitude of the vector difference between winds at 200-hPa and 850-hPa in the main development region of 85°W-15°W, 10°N-20°N during the hurricane season of June-November. To emphasize the multidecadal variability, we first detrend all indices and then perform a 7-year running mean filter to the indices. The correlations of dust with the number of hurricanes and VWS at zero lag are -0.79 and 0.69, respectively.

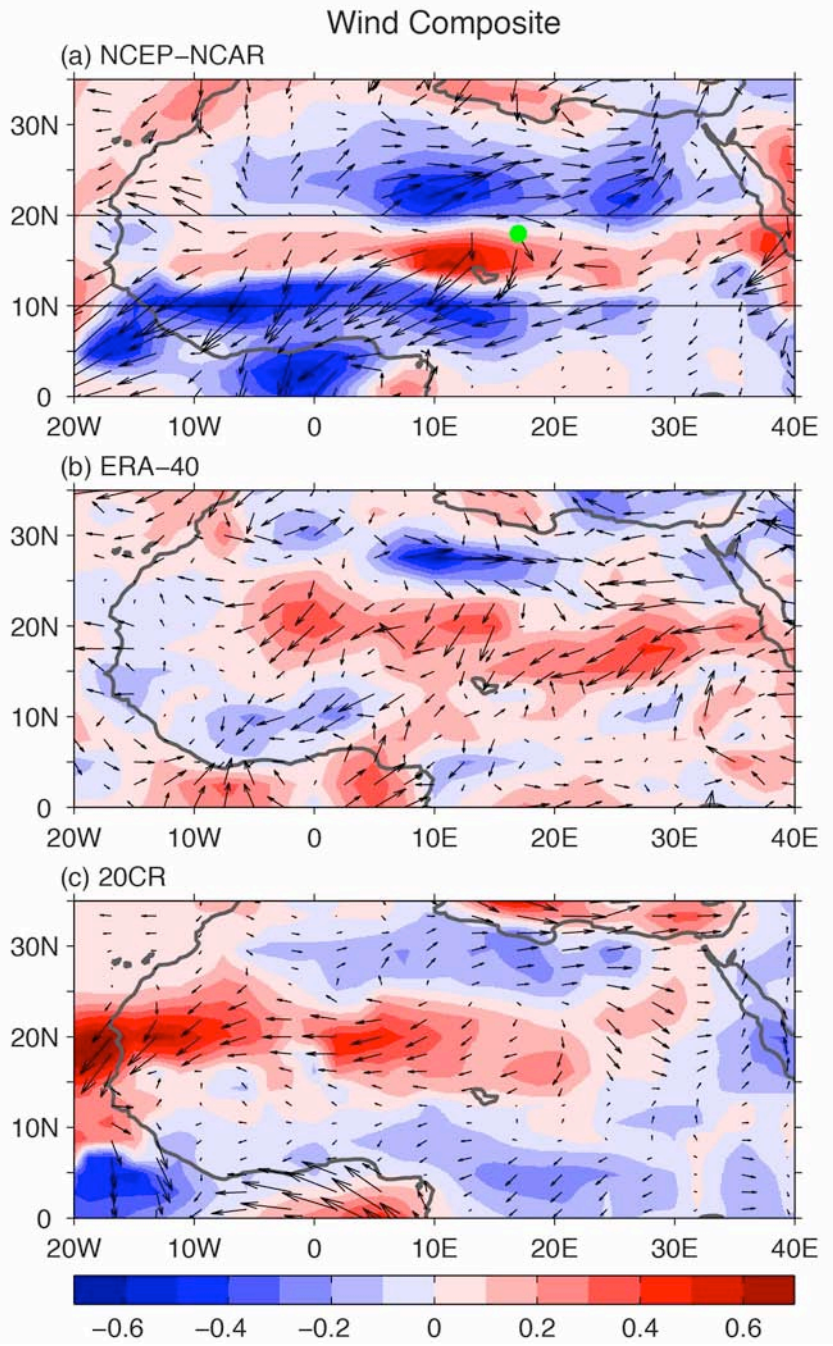

Figure 9. Composite surface wind differences between the high and low dust years. Shown are from (a) the NCEP-NCAR reanalysis, (b) the ERA-40 reanalysis and (c) the 20CR reanalysis. The shading represents the wind speed (m/s). The top and bottom quartiles of the DAOD time series are identified as the high and low dust years, respectively. For the NCEP-NCAR and 20CR, the 13 high dust years are 1962, 1973, 1974, 1975, 1979, 1981, 1983, 1984, 1985, 1986, 1987, 1988 and 1991; and the 13 low dust years are 1955, 1956, 1957, 1958, 1961, 1964, 1976, 1977, 1996, 2003, 2004, 2005, and 2006. For the ERA-40, the 11 high dust years are 1962, 1973, 1974, 1975, 1979, 1981, 1983, 1984, 1985, 1986 and 1987; and the 11 low dust years are 1958, 1961, 1964, 1965, 1968, 1976, 1977, 1993, 1995, 1996 and 2001. The green dot in (a) represents the Bodélé Depression – the lowest point in Chad and the planet's largest single source of dust.

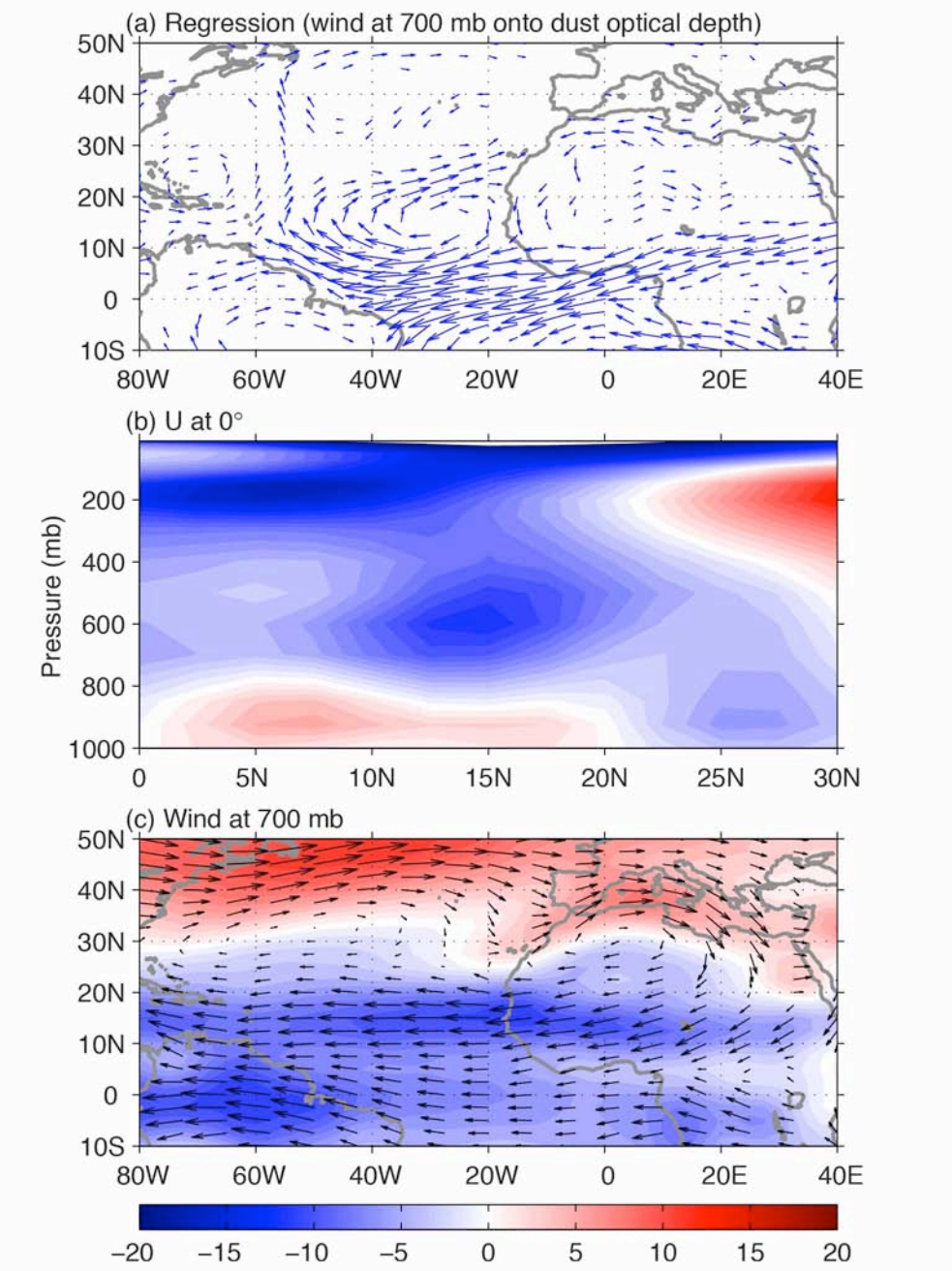

Figure 10. Wind variations with dust and the mean winds. Shown are (a) regression (m/s per DAOD) of annual wind anomalies at 700-hPa onto the DAOD time series, (b) vertical-latitude section of the mean zonal wind at 0° longitude during July-September, and (c) the mean winds (vector) and the mean zonal winds (shading) at 700-hPa during July-September. The regression is calculated based on the detrended and 7-year running mean data. The only regressions exceeding the 95% significant level are plotted.